



Research Article

Misalignment fault detection by wavelet analysis of vibration signals

Özgür Yılmaz^{a,*} , Murat Aksoy^a  and Zehan Kesilmiş^b 

^aDepartment of Electrical and Electronics Engineering, Çukurova University, Balcali Adana, 01380, Turkey

^bDepartment of Electrical and Electronics Engineering, Adana Bilim ve Technology University Saricam Adana, 01380, Turkey

ARTICLE INFO

Article history:

Received 07 August 2018

Revised 13 September 2019

Accepted 10 October 2019

Keywords:

Asynchronous motors

Misalignment fault

Vibration frequency spectrum

ABSTRACT

Asynchronous motors are frequently used in many industrial applications, especially pumps and fans. Placement, bearing and coupling faults are common faults in these types of engines. Misalignment error is a common type of error that is seen very often among these errors. This error may cause efficiency decrease in a short run and vibration may cause short circuit and wear in moving parts in the stator windings in a long run. Early diagnosis of such faults is important in terms of machine health and productivity. In this study, loose connection and angular imbalance of the asynchronous machine were investigated. In the experimental works, a 1 Phase 0.75 KW power asynchronous motor, Y-0036-024A Electromagnetic Brake and SKF Microlog vibration meter were used during the measurements. The Frequency components of motor caused by the settlement errors were investigated under the different loads. A loose assembly error and angular imbalance were investigated from the misalignment errors. The engine was run idle and without any positioning errors and measurements were taken from different points with the accelerometer and the frequency spectrum examined. Measurements are repeated when the misalignment errors are occurred on purpose and the FFT frequency components were compared under the load of 12.50Nm using magnetic brake. The results show that the FFT frequency components are examined and the placement error can be determined with high success and accuracy. It has been found that harmonic components are formed in the frequency spectrum at 25Hz Coefficients. After the settlement error is generated it is seen that, undesired frequency components that are unloaded are lowered under load when the frequency spectra is examined. In this study, theoretical and experimental comparisons of settlement errors are made. Although many errors in this subject are examined in the same publication in general, only the results of the settlement errors are examined specifically as a contribution to the literature. The results and graphs are presented comparatively to the reader's knowledge.

© 2019, Advanced Researches and Engineering Journal (IAREJ) and the Author(s).

1. Introduction

Asynchronous machines are frequently confronted in the industrial world. Today, the engine is the starting point of mechanical movement in many production processes. Today all industrial plants are exposed to asynchronous motors or a derivative or variant. In routine operations, each component generates a mechanical vibration signal at a given frequency even if the machines are operated under normal conditions. The amplitude and frequency of this signal are also related to the component's own material and design parameters, depending on the rotor rotation speed. Changes occur in component frequency characteristics when the motor is not under normal operating conditions or when an error occurs in the components [1,2]. Since vibration values from the outside of the motor are seen as

the sum of the amplitudes at each frequency, it is very difficult to read under normal conditions [3]. Therefore, by dividing the components of the total signal into frequency components, reading the frequency information of the component operating outside normal conditions in the frequency spectrum will provide a faster and easier way to diagnose faults [4]. It is expected that the signal generated in normal conditions will have a vibration frequency and amplitude, the amplitude of the same vibration signal will increase in case of unbalance, sidebands will occur in the case of Settlement Errors, harmonics will be formed with general expression in case of loose connection and bearing errors [5].

The aim of this study is to investigate the frequency response of placement errors of motors. The total frequency is divided into its components by fourier

* Corresponding author. Tel.: +90-322-455 00 40 / 2401.

E-mail addresses: ozgur.yilmaz@gmail.com (Ö. Yılmaz), aksoy@cu.edu.tr (M. Aksoy), zkesilmis@adanabtu.edu.tr (Z. Kesilmiş)

ORCID: 0000-0003-0972-0226 (Ö. Yılmaz), 0000-0002-6980-5902 (M. Aksoy), 0000-0002-5781-9450 (Z. Kesilmiş)

DOI: 10.35860/iarej.451528

transform and the changing frequency component is investigated by the placement error. When this error persists, a torque of 12.5Nm is added as a load on the motor and the same components are examined under load. In the experimental works, an asynchronous motor, Y-0036-024A Magnetic Powder Brake and SKF Microlog CMXA 80 vibration measurement and analysis device were used in 1 Phase 0.75KW power. All researchers worked in the laboratory during experimental studies.

Step 1: Vibration values have been obtained by operating the engine without a load.

Step 2: An angular error was given to the motor and measurements were made in the unloaded position.

Step 3: Measurements were made with a 3° angular placement error.

Many publications in literature, anomalies in vibration signal characteristics have been detected by wavelet analysis. Bearing failures, shaft imbalances and coupling failures have been studied. Bayrak et al. developed a power-based algorithm for the detection of broken rotor rod and concluded that by analyzing the changes in the energy densities of the components in the 90-110 Hz frequency range, the rotor fractures occurring on the motor consisted of components twice the network frequency [1]. Ayaz, E. studied an AI system to detect bearing faults with wavelet analysis. In this study the relationship between motor vibration and current signals was used as training set of an auto-associative recurrent neural network and with this way bearing failure frequencies was determined [6]. Carbajal-Hernández et al. studied the orbital analysis to detect rotor unbalance error to propose a new computational model. In this model it is suggested that vibration signals are processed with suggested computational model to obtain characteristic patterns created by orbits. These patterns are evaluated as inputs to a AI neural network [2]. Chen et al. studied Rotating Machinery Fault Diagnosis (RMFD). Wavelet Analysis was used as the method. The study mainly covers the use of wavelet analysis on RMFD. They also mentioned the advantages/disadvantages of wavelet analysis in different applications and finally made a study for the detection of bearing faults [7].

Although most of the engine failure types and wavelet method have been studied no publication was found to detect misalignment faults by wavelet analysis. The focus of this study is the misalignment faults. The method used in this study is wavelet analysis of vibration signals. With this aspect, the study is thought to contribute to a gap in the literature.

2. Motor Frequency Components

2.1 Fourier Transform

The Fourier transform (FT) is a transformation that allows multiple signals to be expressed as a single total signal and each of these components can be expressed separately in

frequency and amplitude separately from the total signal. Because time information is not carried by the Fourier Transformation, it does not give information about the time of the frequency, but it is used in signals that do not show time dependent changes [8,9].

Fourier Transform can be divided into Continuous Time Fourier Transform (CTFT) and Discrete-Time Fourier Transform (DTFT).

Continuous Time Fourier Transform can be expressed as;

$$F(k) = \frac{1}{\sqrt{2\pi}} \int_{-\infty}^{\infty} f(x)e^{-ikx} dx \quad (1)$$

$$f(x) = \frac{1}{\sqrt{2\pi}} \int_{-\infty}^{\infty} F(k)e^{ikx} dk \quad (2)$$

$$X(e^{j\omega}) = \int_{-\infty}^{\infty} X_c(t)e^{-j\omega t} dt \quad (3)$$

And Discrete-Time Fourier Transform is expressed as;

$$X(e^{j\Omega}) = \sum_{n=-\infty}^{\infty} x[n]e^{-j\Omega n} \quad (4)$$

The discrete-time Fourier transform gives complex exponential signal components at different frequencies of a discrete-time signal. Discrete-time is periodic with 2π period due to the properties of complex exponential signs [8,10].

$$X(e^{j\Omega}) = \sum_{n=-\infty}^{\infty} x[n]e^{-j\Omega n} \quad (5)$$

Inverse discrete-time Fourier transformation expression;

$$x[n] = \frac{1}{2\pi} \int_{-\pi}^{\pi} X(e^{j\Omega}) e^{j\Omega n} d\Omega \quad (6)$$

The Fourier spectrum of a signal is as follows, with amplitude and phase components;

$$X(e^{j\Omega}) = |X(e^{j\Omega})| e^{j\angle X(e^{j\Omega})} \quad (7)$$

The amplitude of the Fourier transform $|X(e^{j\Omega})|$ points out amplitude spectrum and the amplitude spectrum is called the phase $\angle X(e^{j\Omega})$ phase spectrum.

Absolute summability is sufficient to enable fourier transformations of the signals, but Fourier Transform can also be performed when it is not aggregable. In the Fourier transforms, the convergence of the sign transformations in the infinite period is important, so Fourier Transform can also be performed for non-aggregate functions. The amplitude spectrum of the discrete-time $x[n]$ sign is a dual function, and the phase spectrum is a single function. The amplitude spectrum is symmetrical because the $x[n]$ sign is examined in the range $(-\pi, \pi)$. The phase spectrum is reversed-symmetrically. For this reason, it is sufficient to examine the frequency spectrum $(0, \pi)$. This is due to the symmetrical property of Discrete-Time Fourier Transform.

2.2 Frequency Components

Each piece on a running motor creates a vibration. Components such as windings, fans, bearings in the motor

create a component in the frequency spectrum [11]. It is expected that there will be a frequency spectrum like the one in Figure 1 for a motor that works in ideal conditions.

However, other components affecting the frequency components also have different effects on this component. The frequencies of these components are shown in Figure 2 [5,8].

When these components are picked up by the sensor, it looks like Figure 3 in the amplitude-frequency domain.

2.3 Frequency Spectrum Error Components

Each component reflects its frequency on the vibration signal. Therefore, each component generates error signals with different characteristics on the frequency component that it has formed [12-13].

Table 1 shows which faults are caused by faults in these components.

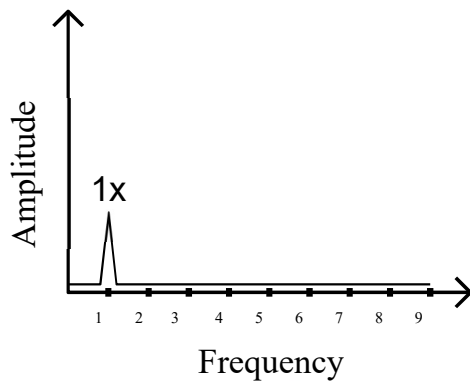


Figure 1. Motor ideal operation frequency spectrum

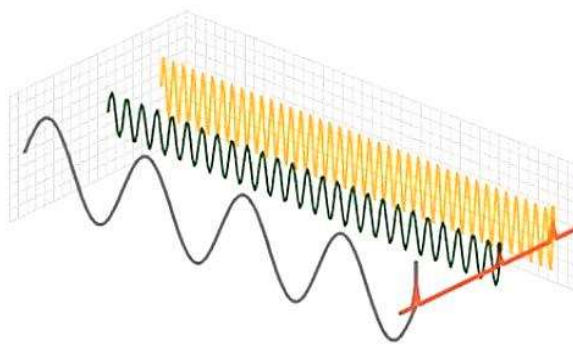


Figure 2. Frequency components

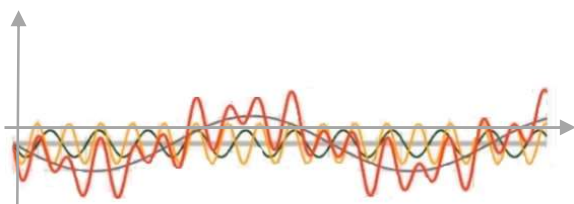


Figure 3. Amplitude-time graph of total vibration signal

Table 1. Error types [3]

Reason for Failure	Parameter Affected by Fault				
	Temperature	Pressure	Leakage	Oil	Vibration
Imbalance					√
Axis Obstruction	√				√
Bearing Load	√				√
Bearing Bed	√	√	√	√	√
Thead Damage				√	√
Looseness					√

Table 1 shows, vibration occurs in all types of error. Figure 1 gives the frequency spectrum expected to occur under ideal conditions. The frequency spectra that occur when errors occur are examined below.

2.3.1 Imbalance

The equilibrium (balance) of all the forces generated by the rotating elements in the machine is called the balance. Any change in this equilibrium causes unbalance. Imbalance is one of the most common types of error that are the most common cause of vibration in machines. Theoretically, no vibrations occur in a perfectly balanced machine. In practice there is no perfectly balanced machine. All machines are unbalanced, even at low levels. This imbalance forms a peak at the vibration frequency (1x) of the shaft rotation speed in the spectrum graph [14]. The components of the erroneous frequency spectrum expected to come into play in the case of imbalance are as shown in Figure 4.

In this graph, the growth of the component in the frequency spectrum in the normal operating mode is expected. The growth affects on the nominal rotation frequency, since the rotor will form once per revolution, due to the static imbalance on the rotor shaft.

2.3.2 Looseness

The working machine parts have loose connections over time. Generally, in the vibration spectrum graph, the vibration generated by the spindle revolution consists of multiple harmonics (1x, 2x, 3x, ...). In some cases, the shaft is also at half harmonics (0.5x, 1.5x, 2.5x, ...) of the revolution [12,14-15].

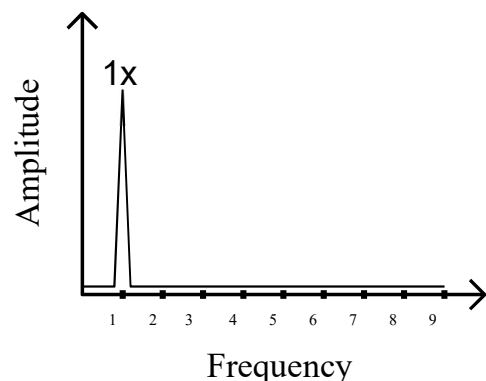


Figure 4. Imbalance frequency spectrum

In the case of a slack error, it is expected that the frequency spectrum of each component will be different in the frequency spectrum, so Figure 5.

Looseness of engine failure as the loose shaft and bearing looseness in the assembly error in the basic work done on the ground should be examined separately [15,16].

2.3.3 Bearing Fault

Roller bearings are widely used in rotating machinery. The problem-free operation of the machines is directly related to the healthy operation of the bearings. Vibration can be measured from the machine bearings and information can be obtained about the developments in the internal structure of the machine [16-17].

There are four types of failure frequencies that characterize the failure in the occurrence of a failure in the bearing. These are the outer ring, the inner ring, the rolling element and the lattice frequency [6,18].

The frequency components for the bearing failures are calculated by the following formula.

$$f_{du} = \frac{n}{2} f_r [1 - \frac{BD}{PD} \cos \beta] \quad (8)$$

Here;

- n = Number of Balls
- $PD = (D_1 + D_2) / 2$
- D_1 = Ball Outside Radius
- D_2 = Ball Inner Radius
- BD = Ball Radius
- f_r = Cycle Frequency
- β = Contact Angle.

It is expected that BPF harmonic components will occur in bearing problems. This is the harmonics that vary depending on the inner and outer diameters of the bearing. The graphical characteristic of the U is expected to occur as shown in Figure 6 [6,19].

2.3.4 Misalignment

Placement mistakes are very common in engine failures. 50% of the failures on systems containing asynchronous motors constitute placement errors.

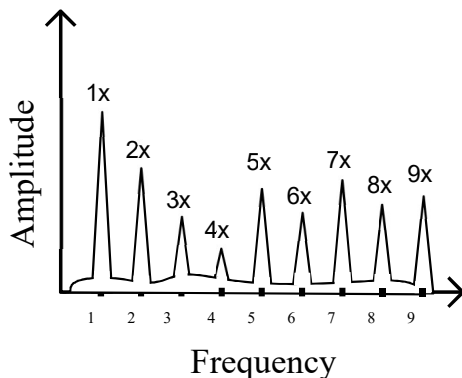


Figure 5. Frequency Spectrum of Looseness Error

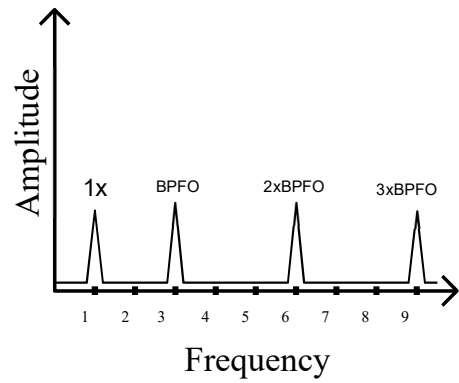


Figure 6. Bearing Failure Frequency Spectrum

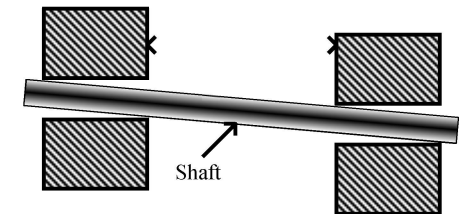
Placement mistakes can be examined in two main sections.
 - Axial Misalignment,
 - Actual Misconception

Axial Distortion It occurs when the spindle, coupling or bearings are not adjusted from their exact centers [6,20]. The cases like Figure 7 are examples of axial misalignment.

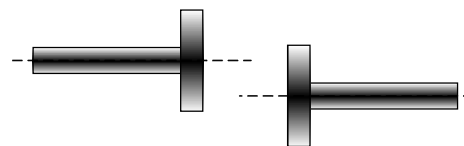
All three types of misalignment cause a significant imbalance in the machine, which causes a vibration in the spectrum graph that causes a peak at 1x frequency. Internal (bearing) and parallel misalignment cause a high peak at 2x harmonic frequency at the same time.

Inner misalignment is a type of error related to the shaft. Parallel misalignment error experimental setup Figure 8 and the drawings of the experimental setup with angular misalignment error are shown in Figure 10.

The frequency response expected from Figure 8 is shown in Figure 9.



a) Inner Misalignment



b) Parallel Misalignment



c) Angular Misalignment

Figure 7. Examples of Axis Misalignment

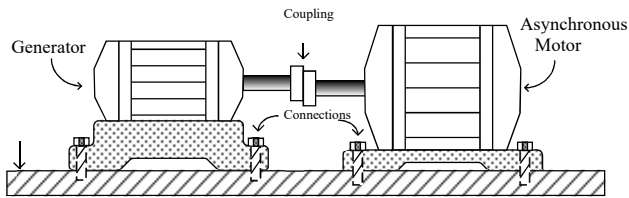


Figure 8. Parallel misalignment error

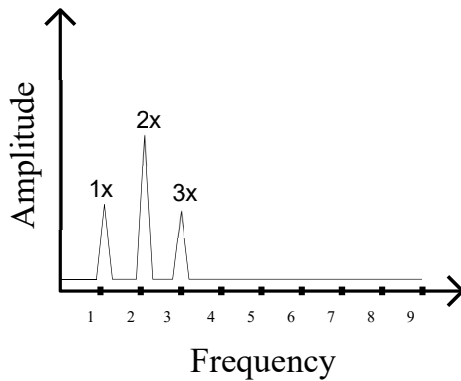


Figure 9. Parallel misalignment error frequency spectrum

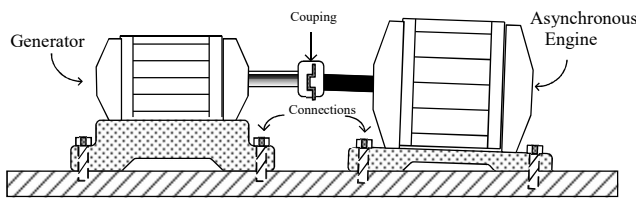


Figure 10. Angular alignment error

Measurements made for angular misalignment are detailed in the measurement results section.

It is expected that the frequency spectrum expected in parallel misalignment mistakes is as shown in Figure 9.

The placement error can also be angular. In this case, it causes an amplitude increase at 1x, 2x harmonic frequencies because it will also cause imbalance on the shaft.

Placement errors and axial misalignments cause a force above the load limit that the bearing can carry. This force on the inner and outer surfaces of the ball bearing and on the ball causes various abrasions and part breaks depending on the time. This causes heating on the ball bearings and therefore on the engine surface. As a result of these warm-ups and wears, motor noise problems and coupling problems due to heat can be seen [6,21].

Another variation of spectrum seen in settlement faults is side band formation.

2.3.4.1 Side Band Formation

The frequency components are two-sided around a central frequency. Despite being bilateral, they are not symmetrical. Carrier occurs depending on frequency. This carrier frequency can be the gear clutch frequency, the ball bearing frequency multiples, the resonance frequency of the machine

or the structure, or the resonance frequency carrier frequency of the acceleration metric [16,21].

The sideband may also be referred to as the modulation frequency. It occurs when a frequency f_1 is modulated by f_2 . For this reason, it is also known by this name.

3. Measurements and Results

3.1 Experimental Setup

Measurements were made in the laboratory environment. The drawings used for the measurements are given below.

Technical specifications for the engine are shown in the Table 2,

Technical specifications for the vibration analyzer are shown in the Table 3,

Technical specifications for load information are shown in Table 4.

Experimental setup including the motor, brake and coupling connection is shown in Figures 11-14.

3.2 Measurements Results

The measurements are based on the front and rear roller bearings of the motor. First, the values obtained without giving any settlement errors were taken and then the values were obtained by giving axial error and slackness errors.

Table 2. Experimental setup engine specifications

Engine Values	
Rated Voltage	230 V, 50 Hz
Velocity	1500 RPM
I_N	4,6 A
I_A / I_N	4.5
T_N	5,10 Nm
$\cos \phi$	0,98
Code	MSD 80 4b

Table 3. Experimental setup analyzer specifications

Vibration Analyzer	
Brand /Model	SKF CMXA 80 Portable Data collector/ FFT Analyzer
Number of Channel	4
I_N :	4,6 A

Table 4. Experimental setup load specifications

Load Informations	
Brand /Model	Y-0036-024A Magnetic Brake
Cycle	4000 RPM
Voltage	24V DC
Current	1,2A
Torque	20Nm

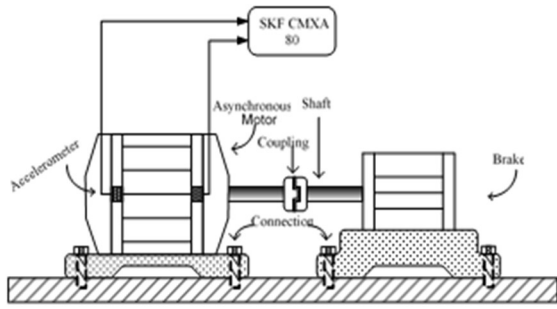


Figure 11. Experimental setup (schematic)

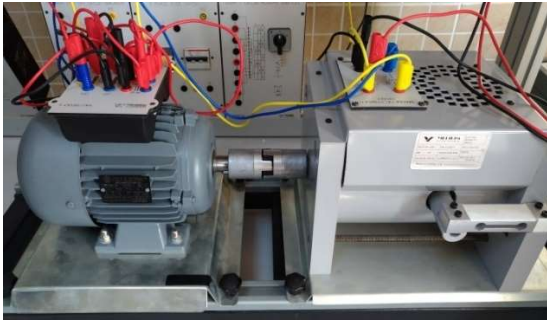


Figure 12. Experimental setup (1st)

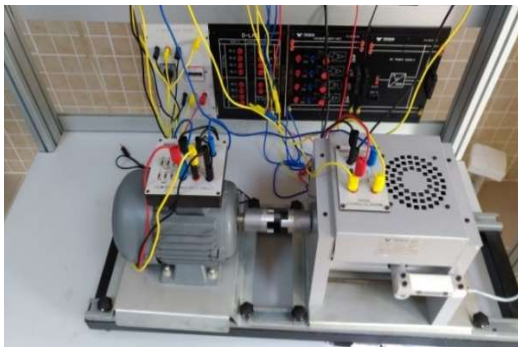


Figure 13. Experimental setup (2nd)

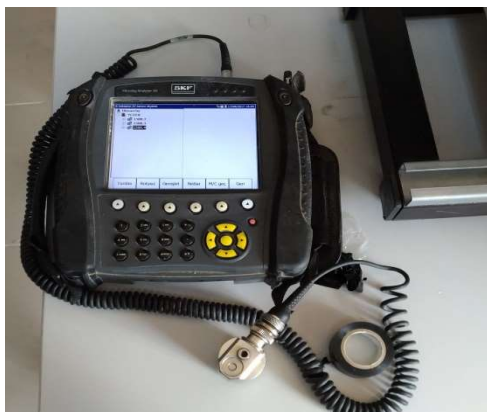


Figure 14. Vibration analyzer (SKF CMXA 80)

The values obtained in the unloaded position of the motor are given in Table 5. Error values in the case of angular imbalance are given in the following tables. The values obtained in the unloaded position by the angular imbalance are given in Table 6. In case of motor 3° angular misalignment fault, measurements were taken under load with torque of 12.5Nm. The values are given in Table 7.

3.3 Frequency Spectrums

The frequency spectra of the values obtained in erroneous and error-free measurements are given below. Natural operation in no-load position When there is 100Hz component in frequency, in case of placement fault, this component increases in amplitude and harmonics are generated at 25Hz frequencies.

The values obtained in the unloaded position of the motor are given in Figure 15. Frequency spectrum when the 3° angular misalignment exists and under load with torque of 12.5Nm is shown in Figure 16.

Table 5. No-load operation Vibration values

Place of Measurement	Date/Time	Last Value	Unit
MFH RUL	17.08.2017 16:03	0,286	gE
MFH HIZ	17.08.2017 16:03	3,62	mm/s
MRH RUL	17.08.2017 16:02	1,329	gE
MRH HIZ	17.08.2017 16:02	2,186	mm/s

Table 6. Unloaded vibration values under angular unbalance

Place of Measurement	Date/Time	Last Value	Unit
MFH RUL	17.08.2017 16:24	0,893	gE
MFH HIZ	17.08.2017 16:24	7,371	mm/s
MRH RUL	17.08.2017 16:23	0,198	gE
MRH HIZ	17.08.2017 16:23	9,986	mm/s

Table 7. Angular imbalance and vibration values under load of 2.5Nm

Place of Measurement	Date/Time	Last Value	Unit
MFH RUL	17.08.2017 16:27	0,708	gE
MFH HIZ	17.08.2017 16:27	4,275	mm/s
MRH RUL	17.08.2017 16:27	0,421	gE
MRH HIZ	17.08.2017 16:26	3,68	mm/s

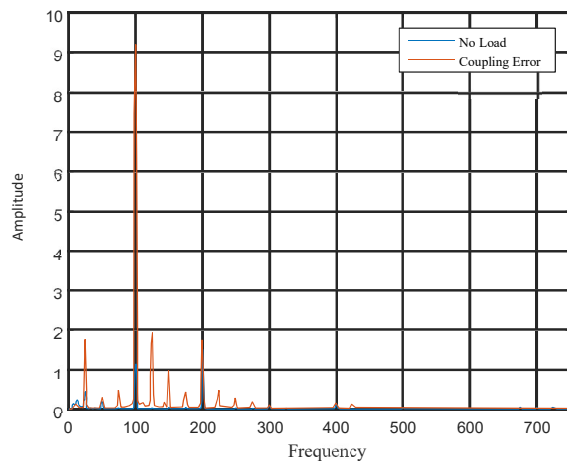


Figure 15. No-Load Operation and 3° Coupling Irregularities Frequency Spectrum

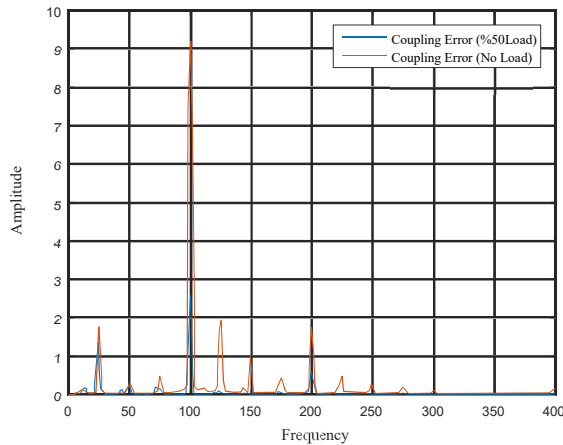


Figure 16: Frequency spectrum at 3° angular imbalance spectrum and under 12.5 Nm load

4. Conclusions

Engine components react to all kinds of abnormal working conditions over time. These reactions may be errors that affect other components in a distributed manner, or a single component connected fault. There is a natural vibration diagram that is generated as a result of the mechanical harmonic motion of each component. As a result of these graphs, the total vibration graph characteristic can be monitored by means of sensors. When this periodic motion is FFT transformed, the frequency component of each motor element can be obtained on the spectrum. These frequency components may vary depending on the rotor frequency and material structure of the mechanical part concerned, depending on external conditions. In case of error, the frequency component reacts like amplitude change, phase shift, harmonic formation, side band formation.

In this study, it was observed that the components of the rotor resonance were found in multiple harmonics such as 1x, 2x in the settlement faults examined (Figure 13) However, side bands are formed. The reason for the formation of these sidebands is that one of the two frequency forming around a center frequency modulates the other frequency.

In this study, the effect of the settlement error on the frequency spectrum has been proved experimentally. Thus, the desired harmonic components are shown graphically to readers.

In the case of angular imbalance in measurement, the value of the amplitude in the unloaded position falls below 12.5Nm under load. This is due to the modulating of the amplitude of the rotor vibration sign of the motor under load. The frequency component is undergoing amplitude modulation unchanged and the amplitude of the vibration signal is reduced.

As a result, it can be said that the settlement error on the motor forms harmonics as an integer number of times and can be observed on the frequency spectrum by sideband formations. The deviation rates in the spectrum have important clues as to the magnitude of the imbalance in settlement error.

Nomenclature

<i>FT</i>	: Fourier Transform
<i>FFT</i>	: Fast Fourier Transform
<i>CTFT</i>	: Continuous Time Fourier Transform
<i>DTFT</i>	: Discrete-Time Fourier Transform
<i>MFH</i>	: Motor Front Half
<i>MRH</i>	: Motor Rear Half
<i>Nm</i>	: Newton.Meter
<i>RPM</i>	: Rate Per Minute

References

1. Bayrak, M., & Küçüker, A., Üç fazlı asenkron motorlardaki kırık rotor çubuğu arizalarının tespiti için güç tabanlı bir algoritmanın geliştirilmesi. *Journal of the Faculty of Engineering and Architecture of Gazi University*, 2014.29(3),303–311. <https://doi.org/10.17341/gummfd.82945>
2. Juan Carbajal-Hernández, J., Sánchez-Fernández, L. P., Hernández-Bautista, I., Medel-Juárez, J. de J., & Sánchez-Pérez, L. A. (2016). *Classification of unbalance and misalignment in induction motors using orbital analysis and associative memories. Neurocomputing*, 2016.175: p.838–850. <https://doi.org/10.1016/j.neucom.2015.06.094>
3. Karahan, M. F., *Titreşim analiziyle makinalarda arıza teşhisi. Yüksek Lisans Tezi, Celal Bayar Üniversitesi Fen Bilimleri Enstitüsü, Manisa,2005:p.37-55.*
4. Cerit, M., *Makine Mühendisliği El Kitabı Cilt 1: Üretim ve Tasarım, TMMOB,1994(169):p.2-32.*
5. Kalyoncu, M., *Titreşim analizi ile makina elemanları arızalarının belirlenmesi. Mühendis ve Makina Dergisi, Ankara,2006.47(552):p.28-35.*
6. Ayaz, E. *Elektrik motorlarında dalgacık analizi yaklaşımı ile rulman arıza tanısı ve yapay zeka tabanlı bir durum izleme sistemi (Doctoral dissertation, Fen Bilimleri Enstitüsü),2001:p.55-62.*
7. Chen, J., Li, Z., Pan, J., Chen, G., Zi, Y., Yuan, J., He, Z., *Wavelet transform based on inner product in fault diagnosis of rotating machinery: A review. Mechanical Systems and Signal Processing*, 2016.70:p.1-35. <https://doi.org/10.1016/j.ymsp.2015.08.023>
8. Abbak, A., *Jeodezide Zaman Dizilerinin Dalgacık (Wavelet) Analizi. Doktora Tezi, Selçuk Üniversitesi, Fen Bilimleri Enstitüsü, Konya,2007:p.8-17.*
9. Chandra, N. H., & Sekhar, A. S., *Fault detection in rotor bearing systems using time frequency techniques. Mechanical Systems and Signal Processing*, 2016.72(73):p.105–133. <https://doi.org/10.1016/j.ymsp.2015.11.013>
10. Patil, SS, Gaikwad, JA, *Vibration analysis of electrical rotating machines using FFT: a method of predictive maintenance. In: 2013 fourth international conference on computing, communications and networking technologies (ICCCNT), Tiruchengode, India, 4–6 July 2013, pp.1–6.*
11. Lu, J., Ming, T., & Zhang, C. (2019). *Simulation Research of Rotor Misalignment Fault Based on Adams. IOP Conference Series: Earth and Environmental Science*, 2019.252(2):p.022148. <https://doi.org/10.1088/1755-1315/252/2/022148>
12. Raj, V. P., Natarajan, K., & Girikumar, T. G. (2013, October). *Induction motor fault detection and diagnosis by vibration analysis using MEMS accelerometer. In Emerging Trends in Communication, Control, Signal Processing & Computing Applications (C2SPCA), IEEE International Conference,2013(2013):p. 1-6.*

13. Thomson, W., *Theory of vibration with applications*. CrC Press,2018:p.17-24.
14. Köse, R. K., *Makine arızalarının belirlenmesinde titreşim analizi*. Mühendis ve Makine Dergisi, 2004(45).538:p:24-32.
15. Cveticanin, L., Vecseri, A., Bíró, I., & Cveticanin, D., *Detection Procedures For Shaft Misalignment detection:An Overview*. Annals of the Faculty of Engineering Hunedoara-International Journal of Engineering,2019.17(1):p.1-4.
16. Ding, H., & Sun, Y.,*Rolling bearing fault feature extraction based on Daubechies wavelet decomposition*. IEEE 37th Chinese Control Conference, 2018:pp.8645-8649.
17. Song, W., Xiang, J., & Zhong, Y. *A simulation model based fault diagnosis method for bearings*. Journal of Intelligent & Fuzzy Systems, 2018.34(6): p.3857-3867.
18. Tezcan, M.,Gökhan, A., Canakoglu, A., Turan, M., *Üç Fazlı Asenkron Motor Tasarımı ve FFT Analizi Three Phase Induction Motor Design and FFT Analysis*, [cited 2019 09 July];Available from: http://www.emo.org.tr/ekler/3f79341d72939e6_ek.pdf
19. Wang, J., Zhao, B., & Zhou, H., *Rolling bear fault recognition based on improved sparse decomposition*. IEEE 37th Chinese Control Conference 2018:p. 5790-5794.
20. Hines, A. J. W., Jesse, S., Edmondson, A., & Nower, D., *Motor Shaft Misalignment versus Bearing Load Analysis: Study Shows Shaft Misalignment Reduces Bearing Life*.Maintenance Technology,1999(April):p.11–77.
21. Kumar, C., Krishnan, G., & Sarangi, S., *Experimental investigation on misalignment fault detection in induction motors using current and vibration signature analysis*. In *Futuristic Trends on Computational Analysis and Knowledge Management (ABLAZE)*, IEEE International Conference,2015:p. 61-66.